Viscous Heating and the Stability of Newtonian and Viscoelastic Taylor-Couette Flows

James M. White and Susan J. Muller

Department of Chemical Engineering, University of California at Berkeley, Berkeley, California and Lawrence Berkeley National Laboratory, Berkeley, California 94720

(Received 24 January 2000)

The effects of viscous heating on the stability of Taylor-Couette flow were investigated through flow visualization experiments for Newtonian and viscoelastic fluids. For highly viscous Newtonian fluids, viscous heating drives a transition to a new, oscillatory mode of instability at a critical Reynolds number significantly below that at which the inertial transition is observed in isothermal flows. The effects of viscous heating may explain the discrepancies between the observed and predicted critical conditions and the symmetry of the disturbance flow for viscoelastic instabilities.

PACS numbers: 47.20.–k, 47.50.+d, 61.25.Hq, 83.10.Ji

We present an experimental study of the effects of viscous heating on the stability of the flow of Newtonian and viscoelastic fluids between concentric, rotating cylinders. The isothermal Taylor-Couette (TC) system has long been a paradigm for studies of stability and transitions for Newtonian fluids; as the rotation rate of the inner cylinder is increased, the purely azimuthal base flow becomes unstable at a critical rotation rate and is replaced by a stationary, axisymmetric vortex flow. This instability is driven by centrifugal effects and thus does not occur if the inner cylinder is held fixed and the outer cylinder is rotated. The critical condition may be expressed in terms of a critical Reynolds number Re_c, and as Re is increased beyond Re_c, the stationary, axisymmetric vortices are replaced by increasingly complex flows through a now well-documented series of transitions [1,2].

In the case of viscoelastic fluids, e.g., dilute solutions of polymers, a purely elastic instability occurs at vanishing Re. Here instability is caused by a coupling of a radial velocity fluctuation to $\theta\theta$-normal (or "hoop") stresses. The instability is unrelated to centrifugal effects and occurs with rotation of either cylinder. The critical conditions may be expressed in terms of a critical Deborah number, a ratio of elastic to viscous forces defined as $\mathrm{De} = \lambda\dot{\gamma}$. Here λ is a characteristic relaxation time for the polymer and $\dot{\gamma}$ is the magnitude of the shear rate. Isothermal linear stability analyses using a bead-spring elastic dumbbell model to describe the polymeric component of the solution predict the disturbance flow is nonaxisymmetric and oscillatory [3–6]. While a purely elastic instability has been documented experimentally in a range of polymer solutions and is indeed independent of which cylinder is rotated, discrepancies between experiments and predictions remain. In experiments, De_c is significantly lower than predicted, unusually long onset times or slow growth rates for the appearance of the instability are observed near the critical condition, and the form of the disturbance flow is always stationary and axisymmetric [7–11].

With regard to nonisothermal effects, the effects of an imposed radial temperature gradient on the Newtonian TC instability have received considerable attention [12–15]. The stability of the base Couette flow is influenced by the interaction of the buoyancy forces with both the centrifugal and the gravitational forces, and Re_c depends on the ratio of the centrifugal to gravitational potentials, the Prandtl number (Pr, the ratio of momentum diffusivity υ to thermal diffusivity α), and the temperature difference between the cylinders (or, equivalently, the Grashof number Gr). It is noteworthy that there are only two experimental studies of radial heating for large aspect ratio geometries in the literature [12,13].

The stability of Newtonian TC flow in which the nonisothermal effects are due to viscous dissipation, rather than an imposed temperature gradient, appears to remain largely unexplored. Kolyshkin and Vaillancourt [16] have numerically studied the related case of uniform internal heat generation; here increasing Pr is destabilizing, but in contrast to the case of imposed radial heating with large temperature gradients, instability is always caused by an axisymmetric mode. Al-Mubaiyedh *et al.* [17] have performed linear stability analyses for viscoelastic fluids with viscous dissipation effects present but without considering buoyancy effects. Viscous dissipation is included through a term in the energy equation of the form $\mathrm{Br}(\tau{:}\nabla\mathbf{v})$, where Br is the Brinkman number, defined as the maximum temperature change due to viscous heating normalized by the controlled wall temperature, τ is the deviatoric stress, and $\mathbf{v}$ is the velocity. This analysis shows that in the viscoelastic case, viscous heating results in a radial stratification of the hoop stresses, which drives a radial secondary flow and leads to a stationary, axisymmetric mode of instability at a critical De and wave number which are in good agreement with experiments. These authors also predict that viscous heating in *Newtonian* fluids can lead to significant destabilization relative to the isothermal case and the most unstable mode may be time dependent (oscillatory) rather than stationary. Increasing Br results in increasing destabilization in both Newtonian and viscoelastic cases. To our knowledge, no experimental reports of destabilization of Newtonian TC flow as a consequence of viscous heating exist in the literature.

 0031-9007/00/84(22)/5130(4)$15.00

Here we present the results of flow visualization experiments on two Newtonian fluids and a viscoelastic fluid. The Newtonian fluids are glycerin and a much lower viscosity, aqueous solution of glycerin. The viscoelastic fluid is a dilute solution of a high molecular weight polyisobutylene (molecular weight $\sim 5 \times 10^6$ g/mole) in a viscous, Newtonian solvent of oligomeric polybutene. The steady shear material functions of the polymer solution were characterized on a Rheometrics RMS-800 Mechanical Spectrometer and are well described by the elastic dumbbell constitutive equation. The solution viscosity is 1.81 Pa s and the characteristic relaxation time for this fluid determined from steady shear experiments is 0.095 s. The viscosities of the glycerin and glycerin-water solution are 1.36 Pa s and 0.069 Pa s, respectively. Values of Pr for each fluid were estimated from literature data to be roughly 24 000, 11 000, and 830, for the polymeric, glycerin, and glycerin-water solutions, respectively.

The TC apparatus has an aluminum inner cylinder of radius $R_1 = 6.299 \pm 0.001$ cm and a precision bore glass outer cylinder of inner radius $R_2 = 7.615 \pm 0.003$ cm; the total inner cylinder length is 40.6 cm and the cylinder axes are aligned with gravity. The inner and outer cylinder walls are held at the same temperature by independent circulators which control the wall temperatures to ± 0.1 °C. The inner and outer cylinders may be independently rotated by high resolution, computer-controlled microstepping motors. Experiments were performed by accelerating one of the cylinders from rest to its final velocity over the course of a few seconds at the start of the experiment. The evolution of the flow at constant Re was then monitored. Experiments were also performed with slow ramps in velocity. Here we present only step tests in velocity which allow us to identify the time scale for onset of instability. Re is defined as $\mathrm{Re} = |\Omega_2 - \Omega_1| R_1 (R_2 - R_1)/\nu$, and Br is defined as $\mathrm{Br} = \eta (R_1 |\Omega_2 - \Omega_1|)^2 / k T_0$, where Ω_1 and Ω_2 are the angular velocities of the inner and outer cylinders, k is the thermal conductivity of the fluid, and T_0 is the reference wall temperature at which all parameters are evaluated. Flow visualization was performed by seeding the test fluid with anisotropic, reflective tracer particles which align with the flow, illuminating the gap (i.e., the r-z plane) with a sheet of laser light, and observing variations in the intensity of the reflected light. Digital images were captured with a charge-coupled device camera and a series of image processing steps were performed to enhance the contrast of the images, which is particularly important for visualizing weak disturbance flows, and to test for evidence of nonaxisymmetry of the flow. Details of both the apparatus and the image processing have been published elsewhere [8].

Initial experiments with the glycerin-water mixture confirmed the rapid onset of stationary, axisymmetric vortices at a critical Reynolds number within 2% of the predictions of linear theory for the case of rotation of the inner cylinder with the outer cylinder held stationary. Images of the gap between the cylinders following a rapid ramp to Re_c shows the familiar, regularly spaced Taylor vortices and a space-time plot, formed by extracting a central line of pixels from sequential digital images of the gap between the cylinders and stacking them vertically reveals regularly spaced, vertical bands corresponding to stationary, axisymmetric vortices. At all $\mathrm{Re} < \mathrm{Re}_c$, the flow remains purely azimuthal, as illustrated by the space-time plot shown in Fig. 1(a). Here at $\mathrm{Re} = 0.179\mathrm{Re}_c$, $\mathrm{Br} = 6.57 \times 10^{-6}$, and $\mathrm{Pr} \approx 830$, the featureless nature of the plot reveals the absence of any stationary or moving structures in the gap, consistent with direct examination of the images of the gap. A space-time plot of an experiment at the same Re for the more viscous glycerin, for which $\mathrm{Br} = 3.59 \times 10^{-2}$ and $\mathrm{Pr} \approx 11\,000$, is shown in Fig. 1(b). This plot represents the same experiment as in Fig. 1(a): The outer cylinder is held fixed and the inner cylinder is accelerated from rest to a value corresponding to $0.179\mathrm{Re}_c$ in a few seconds. A purely azimuthal base flow is initially established but is replaced at about 5.3 min by axisymmetric, axially traveling vortices. The vortices oscillate axially and merge with other vortices during the course of the experiment. A comparison of Figs. 1(a) and 1(b) indicates that the vortex flow is due to destabilization of the centrifugal instability by viscous heating effects. That this disturbance flow is not driven solely by buoyancy induced by viscous heating is demonstrated by Fig. 1(c); here we show an experiment at the same Re, Br, and Pr as in Fig. 1(b), but with centrifugal destabilization absent since the flow is generated by rotation of only the outer cylinder.

A sequence of close-up images of this new disturbance flow is shown in Fig. 2. This figure is at the lowest rotation rate of the inner cylinder at which secondary flows were observed for this fluid. Traveling vortices form approximately 20 min after the onset of shearing of the fluid and move downward at ~ 0.0023 gap widths per s, a rate that is slow compared with the rotation of the inner cylinder. The long onset time for the instability is comparable to that observed in viscoelastic TC experiments [8,9].

A simple analysis of viscous heating in TC flow leads to a time scale of $[R_2 - R_1]^2/\alpha$ to reach a significant fraction of the fully developed temperature profile. For highly viscous fluids, this time scale is typically much larger than the time scale to reach a fully developed velocity profile, $[R_2 - R_1]^2/\nu$, and may be on the order of several minutes. Space-time plots for four velocity step experiments for glycerin are shown in Fig. 3. Figure 3(a) shows the first 36 min of an experiment at $\mathrm{Re} = 0.09\mathrm{Re}_c$; the shearing was continued for a total of two hours and no secondary flows were observed. At a slightly larger Re of $0.126\mathrm{Re}_c$, however, vortices appear throughout the gap in 22 min as shown in Fig. 3(b). This is close to the viscous heating time scale $[R_2 - R_1]^2/\alpha \approx 30$ min for this fluid. At higher Reynolds numbers, the finite growth rate of the new mode of instability leads to shorter onset times, as seen in Figs. 3(c) and 3(d).

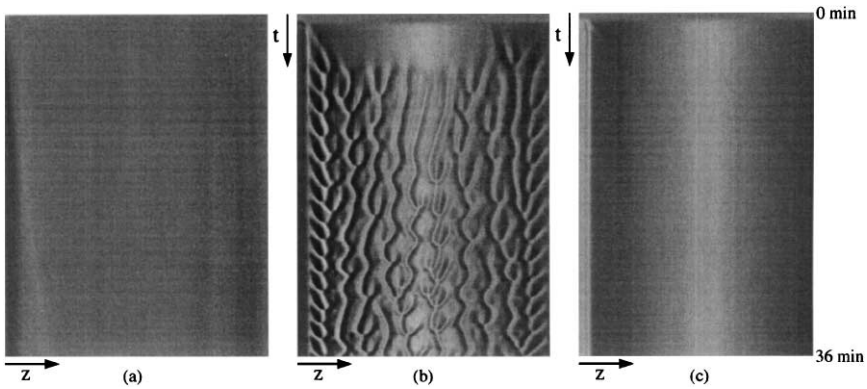

FIG. 1. Space-time plots at $\mathrm{Re}/\mathrm{Re}_c = 0.179$. (a) Glycerin-water, $\dot{\gamma} = 6.0\ \mathrm{s}^{-1}$, $\mathrm{Br} = 6.57 \times 10^{-6}$, with inner cylinder rotating. (b) Glycerin, $\dot{\gamma} = 112.8\ \mathrm{s}^{-1}$, $\mathrm{Br} = 3.59 \times 10^{-2}$, with inner cylinder rotating. (c) Glycerin, $\dot{\gamma} = 112.8\ \mathrm{s}^{-1}$, $\mathrm{Br} = 3.59 \times 10^{-2}$, with outer cylinder rotating. The extent of the z axis is 30 gap widths in each image. In these and all subsequent images, height (z axis) increases to the right.

Figure 4 shows two space-time plots representing velocity step tests for the viscoelastic fluid at $\mathrm{De} = 2.7$, $\mathrm{Re} = 2.7$, $\mathrm{Br} = 6.5 \times 10^{-3}$, $\mathrm{Pr} \approx 24\,000$. These images show a transition from a purely azimuthal shearing flow at short times to a stationary, axisymmetric vortex structure. The vertical streaks indicate that the vortices remain stationary throughout the experiment. The instability is purely elastic as demonstrated by Figs. 4(a) and 4(b): the secondary flow structure is indistinguishable for outer and inner cylinder rotation and is thus independent of centrifugal destabilization. The onset time of 45 min is again roughly consistent with a viscous heating time scale for this viscoelastic fluid.

The experiments pictured in Figs. 1–3 indicate that the new, oscillatory mode of instability in Newtonian TC flow at low Reynolds numbers occurs only above some critical Brinkman number, and only when centrifugal destabilization of the flow is present. Thus, the instability appears to be due to a coupling between viscous dissipation-induced temperature stratification and inertial forces. The observed destabilization of Newtonian TC flow by viscous heating and the change in the form of the disturbance

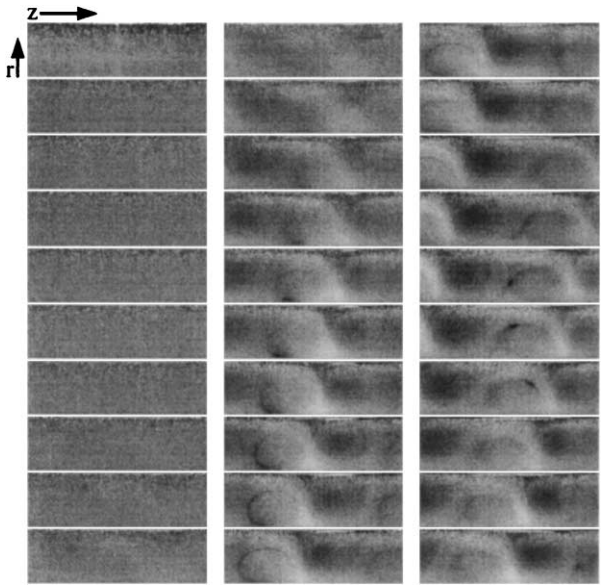

FIG. 2. View of the gap cross section in glycerin at $\dot{\gamma} = 79.1\ \mathrm{s}^{-1}$, $\mathrm{Re} = 12.75 = 0.126\mathrm{Re}_c$, $\mathrm{Br} = 1.77 \times 10^{-2}$, with the inner cylinder rotating. The pictured interval between images is 100 s. The inner cylinder is at the bottom and the outer cylinder is at the top of the images.

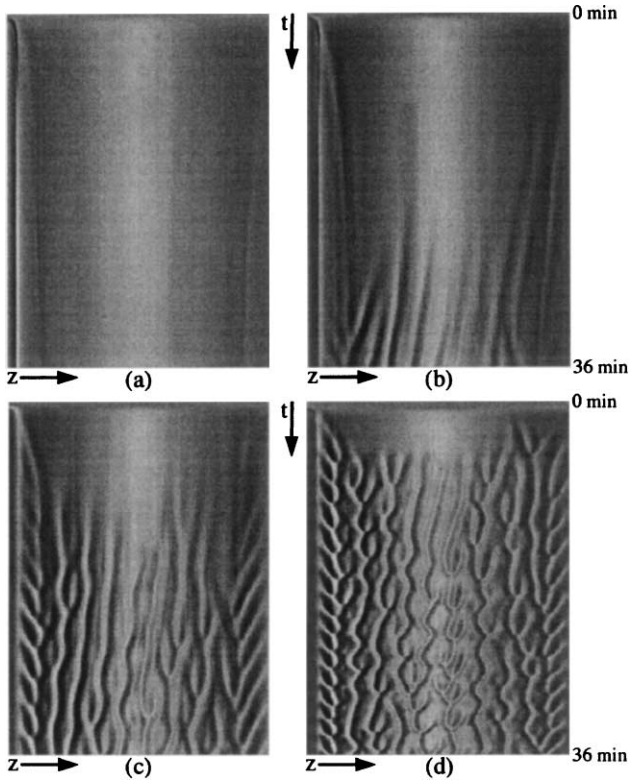

FIG. 3. Space-time plots of glycerin at various rotation rates of the inner cylinder. (a) $\dot{\gamma} = 57.1\ \mathrm{s}^{-1}$, $\mathrm{Re}/\mathrm{Re}_c = 0.09$, $\mathrm{Br} = 9.22 \times 10^{-3}$ (b) $\dot{\gamma} = 79.1\ \mathrm{s}^{-1}$, $\mathrm{Re}/\mathrm{Re}_c = 0.126$, $\mathrm{Br} = 1.77 \times 10^{-2}$ (c) $\dot{\gamma} = 90.2\ \mathrm{s}^{-1}$, $\mathrm{Re}/\mathrm{Re}_c = 0.143$, $\mathrm{Br} = 2.30 \times 10^{-2}$ (d) $\dot{\gamma} = 112.8\ \mathrm{s}^{-1}$, $\mathrm{Re}/\mathrm{Re}_c = 0.179$, $\mathrm{Br} = 3.59 \times 10^{-2}$. The extent of the z axis is 30 gap widths and the outer cylinder is stationary in all images.

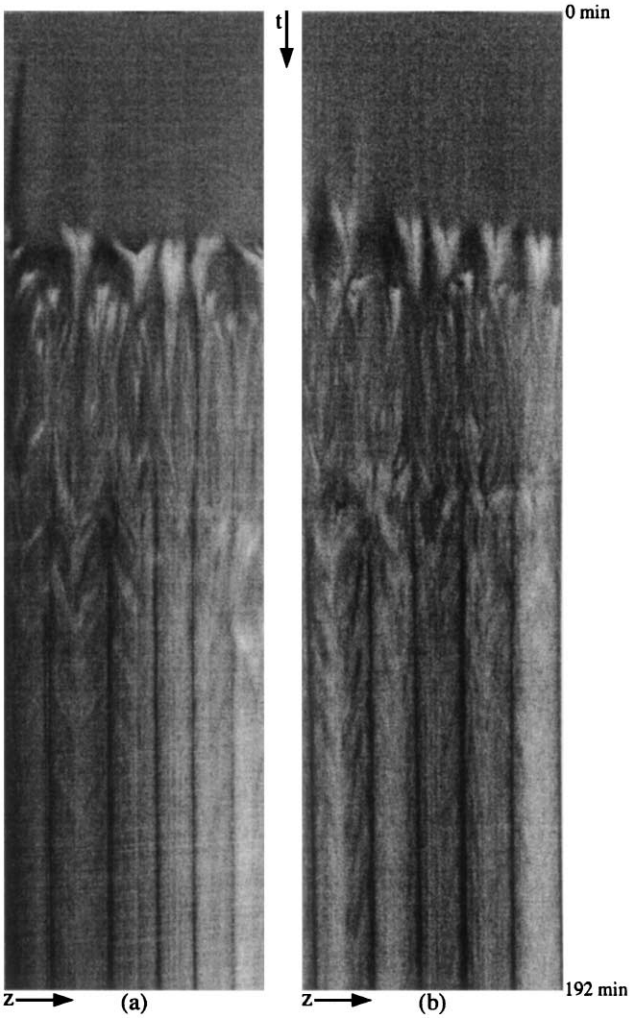

FIG. 4. Space-time plots of the flow of a viscoelastic fluid at $\dot{\gamma} = 30.07\ s^{-1}$, De = 2.7, Re = 2.7, Br = 6.5×10^{-3}, Pr $\approx$ 24 000. (a) Inner cylinder rotating. (b) Outer cylinder rotating. The extent of the z axis is 5.82 gap widths.

flow from stationary to oscillatory with viscous heating are both in good agreement with the recent predictions of Al-Mubaiyedh *et al.* [17]. We attribute the lack of previous reports of this instability to the long time scales before onset of secondary flow, to the high Br (i.e., very high viscosity) required to observe the instability, and to the weakness of the secondary flow.

In the viscoelastic case, the formation of stationary, axisymmetric vortices at the low De depicted in Fig. 4 is inconsistent with isothermal stability predictions. Clearly, if the viscous-heating-induced temperature gradient and resulting radial stratification in fluid physical properties can affect the critical conditions and structure of the Newtonian instability, it may also affect the elastic instability for highly viscous polymeric fluids. These experimental observations again appear to be in good agreement with the viscoelastic linear stability analysis of Al-Mubaiyedh *et al.* [17] in which viscous heating effects are included. We note that the long viscous heating time scale likely also accounts for the anomalously long time scales observed for the onset of viscoelastic instabilities. These onset times are typically several orders of magnitude greater than the characteristic relaxation time of the polymer in solution and were heretofore unexplained. A more detailed experimental study of viscous heating effects in both Newtonian and viscoelastic TC flows in which both the geometry and fluid are varied, as well as a quantitative comparison with stability predictions, is currently in progress. We anticipate viscous heating effects may profoundly affect the stability of industrial polymer processing flows.

This work was supported in part by the Director, Office of Energy Research, Office of Basic Energy Sciences, Materials Science Division of the U.S. Department of Energy under Contract No. DE-AC03-76SF00098.

[1] E. L. Koschmieder, *Bénard Cells and Taylor Vortices* (Cambridge University Press, Cambridge, England, 1993).
[2] R. Tagg, Nonlinear Sci. Today **4**, 1–25 (1994).
[3] R. G. Larson, E. S. G. Shaqfeh, and S. J. Muller, J. Fluid Mech. **218**, 573–600 (1990).
[4] E. S. G. Shaqfeh, Annu. Rev. Fluid Mech. **28**, 129–185 (1996).
[5] Y. L. Joo and E. S. G. Shaqfeh, Phys. Fluids A **4**, 2415–2431 (1992).
[6] M. Avgousti and A. N. Beris, J. Non-Newton. Fluid Mech. **50**, 225–251 (1993).
[7] A. Groisman and V. Steinberg, Phys. Rev. Lett. **77**, 1480–1483 (1996).
[8] B. M. Baumert and S. J. Muller, Phys. Fluids **9**, 566–586 (1997).
[9] B. M. Baumert and S. J. Muller, J. Non-Newton. Fluid Mech. **83**, 33–69 (1999).
[10] A. Groisman and V. Steinberg, Phys. Fluids **10**, 2451–2463 (1998).
[11] R. G. Larson, Rheol. Acta **31**, 213–263 (1992).
[12] H. A. Snyder and S. K. F. Karlsson, Phys. Fluids **7**, 1696–1706 (1964).
[13] M. M. Sorour and J. E. R. Coney, J. Mech. Eng. Sci. **21**, 403–409 (1979).
[14] J.-C. Chen and J.-Y. Kuo, Phys. Fluids A **2**, 1585–1591 (1990).
[15] M. Ali and P. D. Weidman, J. Fluid Mech. **220**, 53–84 (1990).
[16] A. A. Kolyshkin and R. Vaillancourt, Phys. Fluids A **5**, 3136–3146 (1993).
[17] U. A. Al-Mubaiyedh, R. Sureshkumar, and B. Khomami, Phys. Fluids **11**, 3217–3226 (1999).